Proceedings of the 7th GACM Colloquium on Computational Mechanics
for Young Scientists from Academia and Industry
October 11-13, 2017 in Stuttgart, Germany

Mortar-based contact formulations for non-smooth geometries

Alexander Popp[1]*, Philipp Farah[1] and Wolfgang A. Wall[1]

Micro Abstract
Finite deformation frictional contact is revisited with a special emphasis on non-smooth geometries such as corners and edges. Contact conditions are enforced separately for point-, line- and surface-contact by employing three different sets of Lagrange multipliers and a variationally consistent discretization approach based on mortar FE methods. In particular, no unphysical transition parameters are required, but all contact decisions are taken implicitly by the underlying solution scheme.

[1]Institute for Computational Mechanics, Technical University of Munich, Garching, Germany
***Corresponding author**: popp@lnm.mw.tum.de

Introduction

In this contribution, an approach for investigating finite deformation frictional contact problems with a special emphasis on non-smooth geometries such as sharp corners and edges is presented [1]. The contact conditions are separately enforced for point contact, line contact and surface contact by employing three different sets of Lagrange multipliers and, as far as possible, a variationally consistent discretization approach based on mortar finite element methods. The discrete Lagrange multiplier unknowns are eliminated from the system of equations by employing so-called dual or biorthogonal shape functions. For the combined algorithm, no transition parameters are required and the decision between point contact, line contact and surface contact is implicitly made by the variationally consistent framework. To the best of the authors' knowledge, this is not possible with any other mortar-based approach from the literature [2, 3].

1 Problem Definition

Our starting point for deriving the problem formulation is the consideration of two bodies $\mathcal{B}^{(1)}$ and $\mathcal{B}^{(2)}$ with one shared contact interface. The special focus of this contribution is to investigate contact situations involving non-smooth geometries. Therefore, the potential contact boundaries $\Gamma_\mathrm{c}^{(i)}$ are divided into three disjoint subsets, viz.

$$\Gamma_\mathrm{c}^{(i)} = \Gamma_\circ^{(i)} \cup \Gamma_\shortmid^{(i)} \cup \Gamma_\star^{(i)}, \tag{1}$$

$$\Gamma_\circ^{(i)} \cap \Gamma_\shortmid^{(i)} = \Gamma_\circ^{(i)} \cap \Gamma_\star^{(i)} = \Gamma_\shortmid^{(i)} \cap \Gamma_\star^{(i)} = \emptyset, \tag{2}$$

where $\Gamma_\circ^{(i)}$ are the potential contact boundaries of surfaces, $\Gamma_\shortmid^{(i)}$ represent edges and $\Gamma_\star^{(i)}$ are the sets of all vertices within the contact boundaries. In a general finite deformation setting, the geometrical contact entities, namely surfaces, edges and vertices, could deform significantly, meaning that an initial vertex could be flattened to become part of a new surface, or a surface could be deformed in such a way that a new edge is created. However, in this contribution it is assumed that the spatial points are assigned to the set definition of its reference boundary and consequently extreme deformations, such as a complete flattening of an edge, are not allowed. In order to define suitable contact conditions the possibly arising contact scenarios have to be specified. For this purpose, it is assumed that the contact entity with the lower geometrical

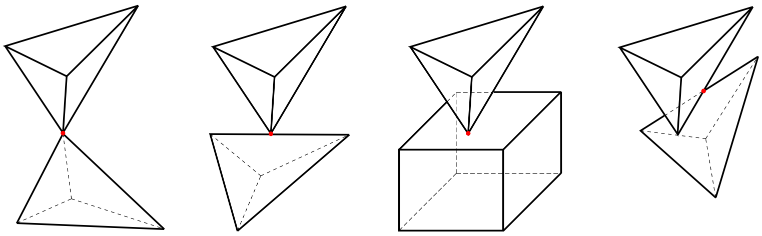

Figure 1. Classification of contact scenarios leading to point contact. From left to right: vertex-to-vertex, vertex-to-edge, vertex-to-surface and non-parallel edge-to-edge. Contact point is highlighted in red.

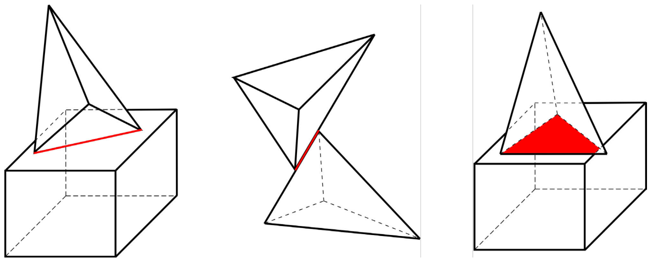

Figure 2. Classification of contact scenarios leading to line contact: edge-to-surface (left) and parallel edge-to-edge (middle). Contact line is highlighted in red. Classical surface contact scenario (right).

dimension acts as slave part and the corresponding contact entity of equal or higher geometrical order is defined to be the master boundary. Concretely, the first class of possible contact scenarios is characterized by the active contacting area reducing to a point, see Figure 1. Namely, these scenarios are vertex-to-vertex, vertex-to-edge, vertex-to-surface and non-parallel edge-to-edge settings. These contact situations are denoted as point contact in the following. The next class is defined by the contacting area being a one-dimensional line, which could arise due to edge-to-surface and parallel edge-to-edge contact, see Figure 2. The last setting is the classical surface contact scenario, which is quite well-investigated and also schematically visualized in Figure 2. This classification represents a hierarchy of contact situations, where the contact boundary on which the contact constraints are going to be formulated is the involved slave entity with the lowest dimension. The only exception to this scheme is the non-parallel edge-to-edge contact. Here, the geometrical slave entity is an edge but the contact scenario reduces to a point contact, which needs to be treated with a penalty regularization.

2 Modification of Discrete Lagrange Multiplier Spaces

One core ingredient of the proposed mortar-based contact formulation for non-smooth geometries is a suitable modification of the discrete Lagrange multiplier spaces for line contact and surface contact in the vicinity of non-smooth geometric entities such as vertices and edges, respectively. This section gives a short exemplary overview of how this modification is achieved for dual (biorthogonal) mortar methods in the case of line contact, i.e. with a 1D Lagrange multiplier for constraint enforcement. The interpolation of the discrete line Lagrange multipliers reads

$$\boldsymbol{\lambda}_{\mathrm{l},\mathrm{h}} = \sum_{j=1}^{n_{\mathrm{l}}^{(1)}} \Theta_j \, \boldsymbol{\lambda}_{\mathrm{l},j} \ . \tag{3}$$

The shape functions Θ_j are based on the finite element parameter space for one-dimensional curves ξ_{l}. The discrete line Lagrange multipliers are carried by the nodes $n_{\mathrm{l}}^{(1)}$, which are defined on physical slave edges except for the nodes $n_{\star}^{(1)}$ attached to vertices. Basically, there are two different types of Lagrange multiplier interpolation. First, so-called standard shape functions can be employed, which are identical to the displacement interpolation of a 2-node line element. Second, shape functions based on a biorthogonality condition can be utilized, which are also commonly known as dual shape functions. These dual shape functions are very advantageous, since they allow for a computationally efficient condensation procedure of the discrete Lagrange multipliers. If a line element is connected to a vertex, it would now carry one discrete line Lagrange multiplier and one discrete point Lagrange multiplier. Thus, partition of unity would not be guaranteed anymore. In order to guarantee partition of unity for these elements, the line Lagrange multiplier shape functions have to be modified in the vicinity of the vertex node, see Figure 3. Here, modification of the dual shape function of the line Lagrange multiplier yields

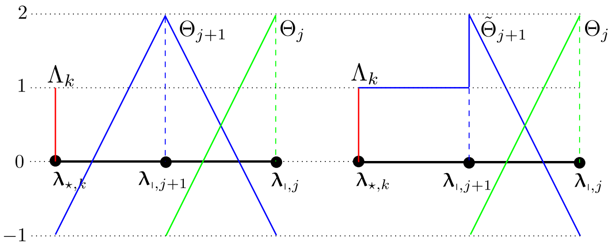

Figure 3. Modification of line Lagrange multiplier interpolation for dual shape functions due to the presence of a point Lagrange multiplier: unmodified shape function (left) and modified shape function (right). The point Lagrange multiplier is visualized as 1 impulse.

a constant interpolation to the point Lagrange multiplier. The modified shape functions are denoted by $\tilde{\Theta}_j$. It should be pointed out that such modifications are quite well-established in mortar finite element methods in the context of Dirichlet boundary conditions or so-called crosspoints, which arise when multiple mortar subdomains meet at one point [4, 5]. Similar modifications of the discrete Lagrange multipliers have also been devised for surface contact.

3 Numerical Example

The numerical example is utilized to exemplarily demonstrate the consistent transition between point, line and surface contact. To this end, an elastic plate is pressed against a rigid foundation. The problem setup is visualized in Figure 4. The plate is meshed with $70 \times 70 \times 3$ tri-linear hexahedral elements with enhanced assumed strain (EAS) element technology. The initial distance between the bodies at their closest points is $d = 0.1$. The nodes at the edge A, which points in thickness direction of the plate, are only allowed to move in Z-direction and the nodes at edge B are subjected to a prescribed total motion of $d_{\max} = 0.72$ in negative Z-direction, which is enforced within 35 steps. Obviously, the first contact occurs at the vertex node at the lower end of edge A. In step 8, the active contact set increases with the adjacent edge nodes becoming active. In step 10, the vertex node eventually becomes inactive and the corresponding point Lagrange multiplier takes on a zero value. Nevertheless, the contact tractions still keep their maximum at the vertex node due to the two active edge nodes and their modified shape functions, see Figure 3. The absolute value of the tractions further decreases since the stresses

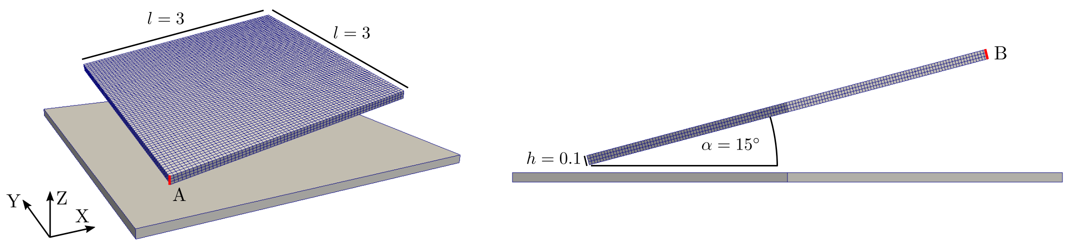

Figure 4. Setup for the bending plate example.

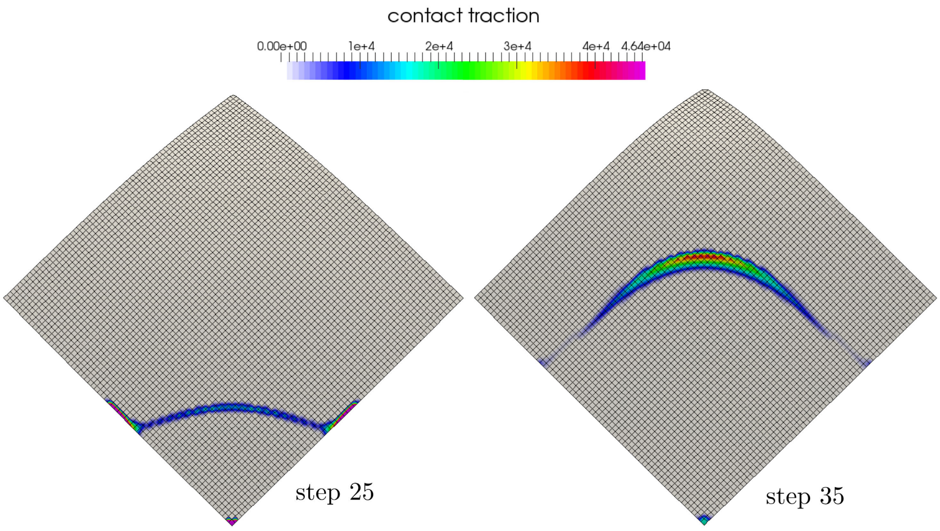

Figure 5. Contact tractions for the bending plate example.

are continuously shifted from the vertex node to the edge nodes. Then, in step 21, the first active surface nodes occur, and the active surface area completely connects the two active edge sectors in step 25, see Figure 5. Interestingly, however, the two edge nodes connected to the vertex node on edge A are still in contact and the highest contact tractions still occur at this region. During the following steps, the region of active surface nodes continuously moves towards edge B and the maximum surface stress values increase. Moreover, the number of active edge nodes reduces and the contact tractions at the edge nodes as well as at the vertex node further decrease. While only being of qualitative nature, this example nevertheless nicely demonstrates the ability of the proposed algorithm to switch smoothly and robustly between point, line and surface contact formulation without any heuristic transition parameter.

Conclusions

A combined framework for frictional point contact, line contact and surface contact based on mortar finite element methods has been discussed. Three sets of Lagrange multipliers represent point, line and surface contact, and no heuristic transition parameters are required to switch between these three sets. Quite in contrast, the transition between point, line and surface contact arises automatically from the underlying, variationally consistent problem formulation.

References

[1] P. Farah, W. A. Wall, and A. Popp. A mortar finite element approach for point, line and surface contact. *Preprint*, submitted for publication, 2017.

[2] A. Popp, M. Gitterle, M. W. Gee, and W. A. Wall. A dual mortar approach for 3D finite deformation contact with consistent linearization. *International Journal for Numerical Methods in Engineering*, 83(11):1428–1465, 2010.

[3] A. Popp, A. Seitz, M. W. Gee, and W. A. Wall. Improved robustness and consistency of 3D contact algorithms based on a dual mortar approach. *Computer Methods in Applied Mechanics and Engineering*, 264:67–80, 2013.

[4] B. I. Wohlmuth. *Discretization methods and iterative solvers based on domain decomposition.* Springer-Verlag Berlin Heidelberg, 2001.

[5] B. I. Wohlmuth. Variationally consistent discretization schemes and numerical algorithms for contact problems. *Acta Numerica*, 20:569–734, 2011.